Response to Reviewer #1:

The paper presents an interesting analysis of measured absorption enhancement by black carbon particles mixed with other species. The data are interesting and quite valuable. However, several aspects of the manuscript are not well explained, and some are confusing or unclear. I think the authors can address most of these shortfalls, and if so, then the manuscript would deserve publication.

General comments

[Comment 1] The definition of "transition state" is vague, and it should be quantified. The criteria used are not clear.

Response: We appreciate the reviewer's insightful comment. In the revised manuscript, we have clarified the definition and usage of the term "transition state". We now explicitly describe it as a case dependent range in which BC particles becomes more compact and thoroughly coated, gradually transitioning toward a core-shell structure. This corresponding text has been revised as follows (Lines 355-363):

"*As M_R increases, $C_{sca\_measured}/C_{sca\_modeled}$ also increases, indicating the BC particles becomes more compact and more thoroughly coated, transitioning toward a core-shell structure (Corbin et al., 2023). Following previous studies (Liu et al., 2017a; Liu et al., 2020), we describe this stage as a "transition state". In this work, the transition state is neither defined by a fixed M_R threshold nor by any directly observed morphological boundary. Instead, it reflects an optically inferred state in which scattering enhancement increases markedly, with M_R ranges of 1.78-6.34 (Case 1), 1.43-3.78 (Case 2), and 1.45-4.19 (Case 3).*"

This clarification provides a more operational and quantitative definition consistent with the observed variability among different cases.

[Comment 2] How the three cases (1,2, and 3) were defined is not clear.

Response: We appreciate the reviewer's valuable comment. In the revised manuscript, we have clarified the criteria to define the three cases (Lines 265-282). Specifically, the classification was based on the temporal variation of the measured E_{abs}, with E_{abs} = 1.5 selected as the reference threshold, as described below:

"To investigate the temporal evolution of BC coating, the observation period was classified into three cases based on the variation of $E_{abs\_measured}$, using E_{abs}=1.5 as the reference threshold (Fig.1). Case 1 (September 3-23 and October 1-7, 2023) corresponds to $E_{abs\_measured}$ significantly below 1.5. These periods were characterized by relatively low non-refractory PM_1 concentrations and high wind speeds (WS = 0.94 ± 0.04 m/s). Back-trajectory analysis further shows that Case 1 was dominated by clean marine and nearby local air masses, resulting in relatively clean and weakly aged conditions (Fig. 1a). Case 2 (September 24–30) corresponds to periods when $E_{abs\_measured}$ remained continuously higher than 1.5. This episode occurred under stagnant meteorological conditions-characterized by weak winds (WS = 0.81 ± 0.02 m/s) and elevated relative humidity (RH = 81.34 ± 17.12%) -that favored secondary aerosol formation. Back-trajectory analysis further indicates that Case 2 was dominated by air masses transported from Jiangsu and passing through

northern Zhejiang, enhancing pollutant accumulation and promoting more aged BC conditions. Case 3 includes periods when $E_{abs\_measured}$ persistently fluctuated around 1.5. The air masses during this period were a mixture of polluted inland outflow and clean marine inflow, suggesting the air masses were moderately aged–which explains the intermediate E_{abs}."

[Comment 3] The link with local conditions, pollution level, and contribution from different sources is not well developed. It is probably possible and relatively straightforward for the authors to use existing monitoring data to corroborate some of their discussions. I would also suggest generating some more discussion of the back-trajectory simulations to determine transport path and time, and potential sources. The authors do show some of this work in the SI, but in the main paper, there is little to no mention, and more discussion should be added.

Response: We thank the reviewer for this insightful comment. We agree that linking our observations with local pollution conditions and potential source influences can strengthen the interpretation of BC absorption enhancement. Although source attribution is not the primary focus of this study, we have incorporated additional analyses to address the reviewer's concerns.

First, we added a discussion connecting the observed E_{abs} variations with concurrent aerosol pollution levels and meteorological conditions (Lines 264-281). These additions help contextualize the measured M_R and E_{abs} under different air-quality regimes. Second, in response to the reviewer's suggestion, we expanded the discussion of air-mass transport pathways in the revised manuscript. Specifically, we performed supplementary 48-hour back-trajectory simulations at 100 m, 500 m, and 1000 m above ground level (Fig. 1c and Fig. S7), and the results consistently show similar transport pathways for different observation periods. These findings indicate that the polluted air masses during Case 2 passed through northern Zhejiang, supporting the interpretation that regional-scale transport contributed to the elevated aerosol loading and high M_R and E_{abs} conditions. A brief discussion of these results has now been included in Section 3.3 (Lines 439-448).

Overall, these additions help strengthen the link between pollution level, transport conditions, and the observed optical properties of BC while maintaining the central focus of this work.

Lines 264-281: *"To investigate the temporal evolution of BC coating, the observation period was classified into three cases based on the variation of $E_{abs\_measured}$, using E_{abs}=1.5 as the reference threshold (Fig.1). Case 1 (September 3-23 and October 1-7, 2023) corresponds to $E_{abs\_measured}$ significantly below 1.5. These periods were characterized by relatively low non-refractory PM_1 concentrations and high wind speeds (WS = 0.94 ± 0.04 m/s). Back-trajectory analysis further shows that Case 1 was dominated by clean marine and nearby local air masses, resulting in relatively clean and weakly aged conditions (Fig. 1a). Case 2 (September 24–30) corresponds to periods when $E_{abs\_measured}$ remained continuously higher than 1.5. This episode occurred under stagnant meteorological conditions-characterized by weak winds (WS = 0.81 ± 0.02 m/s) and elevated relative humidity (RH = 81.34 ± 17.12%) -that favored secondary aerosol formation. Back-trajectory analysis further indicates that Case 2 was dominated by air masses transported from Jiangsu and passing through northern Zhejiang, enhancing pollutant accumulation and promoting more aged BC conditions. Case 3 includes periods when $E_{abs\_measured}$ persistently fluctuated around 1.5. The air masses during this period were a mixture of polluted inland outflow and clean marine inflow, suggesting the air masses were moderately aged–which explains the intermediate E_{abs}."*

Lines 433-443: "*During Case 2, the high aerosol loading and elevated bulk-averaged M_R were largely influenced by regional transport, as air masses at 100 m, 500 m, and 1000 m all followed similar pathways from the northern Yangtze River Delta into northern Zhejiang (Fig. 1c and Fig. S7). Stagnant meteorological conditions, elevated relative humidity, and enhanced oxidative capacity further facilitated vigorous liquid-phase and photochemical reactions, promoting the abundant formation of secondary coatings on BC surfaces (Peng et al., 2016). Notably, our observations show that E_{abs} increases systematically with the increasing contribution of secondary nitrate (Fig. S8), consistent with the fact that nitrate-rich conditions enhance aqueous-phase oxidation and accelerate the formation of thick inorganic coatings (Liu et al., 2017b).*"

[Comment 4] The SI also shows an ACSM, which might provide further information that I did not see discussed in the paper. Maybe I missed it, but was Figure S7 based on the ACSM data? Maybe that could be made clearer in the SI as well as in the main text. Small note: In the same figure, CPAS should be CAPS (?)

Response: We thank the reviewer for this comment. Fig. S7 has now been updated to Figure 1, , and the non-refractory components are based on the ACSM-X measurements. We have clarified this both in the revised manuscript (Lines 145-149) and the Figure 1 title (Lines 301-303) to make it explicit.

Lines 145-149: "*The mass concentrations of non-refractive OA, nitrate, sulfate, ammonium and chloride was measured by time-of-flight aerosol chemical speciation monitor with extended resolution (ToF-ACSM X, Aerodyne). Instrument principles, calibration procedures, and operational details for the ToF-ACSM X are described in a previous study of ours (Zhang et al., 2025).*"

Lines 301-303 "*The time series of BC concentrations, bulk-averaged M_R, measured E_{abs}, and the chemical components (including organics, nitrate, sulfate, ammonium and chloride) measured by TOF-ACSM X, as well as relatively humidity (RH).*"

Regarding the small note, "CPAS" in the figure has been corrected to "CAPS."

[Comment 5] It is not clear to me what the "improved model" is and how it is operationally defined. More details should be provided on this topic as it seems to be central to the discussion.

Response: We appreciate the reviewer's comment. In the revised manuscript, we have explicitly clarified what the "improved model" refers to and how it is operationally defined. The revised manuscript now provides a concise description of the observationally constrained parameterization. These details are now clearly stated in the revised manuscript (Lines 464-495).

"*In this study, we introduce an observationally constrained parameterization that links SP2-measured scattering cross sections with core-shell Mie calculations. This scheme identifies the optical transition state through following steps: (1) measuring single-particle C_{sca} with SP2, (2) fitting the relationship between $C_{sca\_measured}$ and M_R (Fig. 4b-4c), (3) identifying the M_R range associated with transitional optical behavior ("transition state"), and (4) inferring the MAC of transition-state particles using the fitted relationship before integrating MAC over all particles to obtain bulk E_{abs}. This parameterization improves agreement with observations, especially during clean periods (Case 1), when the uniform core-shell assumption tends to produce the largest*

discrepancies. However, its performance depends on correctly identifying the M_R range of the transition state. Our results show that, in polluted periods (Cases 2 and 3), the M_R range associated with the transition-state becomes relatively narrow, while under clean conditions it tends to expand. Consequently, applying a fixed M_R threshold across all atmospheric conditions can introduce systematic biases in modeled E_{abs} (Fig. 4b, c and d). Although M_R heterogeneity alone can adequately reproduce E_{abs} during polluted periods, adopting separate input schemes for different environments would complicate radiative transfer calculations and limit broader applicability.

To address this issue, we emphasize that the proposed framework is adaptable to environments in which BC particles undergo similar optical transitions. Key parameters, including the M_R thresholds that define the transition state and other indicators derived from the $C_{sca\_measured}$-M_R relationship, can be recalibrated for different atmospheric contexts. This includes rural aeras, biomass-burning regions, or seasons with distinct pollution characteristics, where coating composition and aging processes may vary. Although the parameterization is fundamentally based on the optical evolution of BC from loosely coated to more compact states, it can be adjusted to account for local differences in particle coating and aging dynamics. Thus, the unified scheme incorporates both M_R variability and optical characteristics of transitional particles, providing a flexible and physically consistent approach for a wide range of atmospheric environments. Overall, this observationally constrained approach offers a more consistent representation of BC mixing states across diverse atmospheric conditions, thereby reducing uncertainties in optical modeling and enhancing the reliability of BC radiative effect assessments."

[Comment 6] The literature cited is somewhat lacking and perhaps a bit biased; especially lacking is the comparison with other single-particle techniques such as microscopy.

Response: We thank the reviewer for this valuable comment. We acknowledge that direct comparisons with single-particle microscopy observations were not included in this study. Nevertheless, we have now incorporated relevant references in the Introduction to provide additional context on the coating characteristics of ambient BC (Lines 47-59). Although microscopy techniques are not employed here, these studies highlight the variability of coating structures and the limitations of assuming idealized core–shell configurations when modeling BC absorption enhancement. This addition strengthens our discussion on the model assumptions relative to existing observational evidence and better situates our work within the framework of previous single-particle studies.

"*This discrepancy mainly stems from the oversimplified assumptions in Mie theory, which fail to capture the real atmospheric complexity in BC size distribution, coating configuration, and mixing state (Wang et al., 2021b). Previous microscopy-based single-particle studied (e.g., TEM and SEM) have visually demonstrated that the ambient BC particles exhibit diverse coating structures and highly heterogeneous mixing states, providing direct evidence of deviation from the idealized core-shell assumption (Adachi et al., 2010; Adachi and Buseck, 2013; China et al., 2013; Wang et al., 2021b). Although microscopy techniques are not employed in this work, these findings highlight the importance of realistically representing BC mixing state and coating characteristics when modeling optical properties. The mismatch between model assumptions and observations has motivated efforts to refine the conceptual modeling approaches for BC aging and coating evolution, which forms the focus of this study.*"

[Comment 7] Even though the paper is mostly clearly written, the grammar should still be improved; some limited examples are provided in the next section.

Response: We thank the reviewer for this comment. We have carefully proofread the manuscript and improved the grammar throughout the text. In addition, we have addressed the specific examples provided by the reviewer to ensure clarity and correctness of the language.

Specific comments

[Comment 8] Line 35: space after models

Response: Corrected.

[Comment 9] Line 51. I think Fierce's paper also discussed the effect of morphological deviations at low MR

Response: We thank the reviewer for this valuable suggestion. We have revised the manuscript to explicitly acknowledge that Fierce et al. (2020) discussed the effect of morphological deviations from the idealized core-shell structure, particularly at low M_R, on BC E_{abs}, described as follows (Lines 60-66):

"A number of studies have explored the discrepancies in BC E_{abs} from various perspectives. Particle-resolved modeling has demonstrated that both particle-to-particle heterogeneity in M_R and deviations from the idealized core-shell structure can strongly influence absorption estimates (Fierce et al., 2020). In particular, non-uniform or partial coatings at low M_R can lead to the overestimation of E_{abs} by traditional core-shell models. However, these factors alone tend to cannot explain the low E_{abs} frequently observed under high M_R conditions (Huang et al., 2024)."

[Comment 10] Line 86: "an BC" -> "a BC"

Response: Corrected.

[Comment 11] Line 111: "was" -> "were"

Response: Corrected.

[Comment 12] Line 120: How were the concentrations of PSL measured?

Response: We thank the reviewer for the comment. The purpose of using PSL spheres was not to measure their number concentration, but to determine their scattering cross section. Monodisperse PSL particles of different diameters were selected using a DMA and introduced into the instruments, allowing the scattering cross section to be measured for calibration purposes. This clarification has been added to the revised manuscript (Lines 164-171):

"*Besides, before sampling, the scattering coefficient of CAPS-ALB and Nephelometer at every wavelength was calibrated using PSL spheres. Monodisperse PSL particles of different diameters (100 nm, 150 nm, 200 nm and 300 nm) were selected using a Differential Mobility Analyzer (DMA) and introduced into the instruments, enabling accurate measurement of their scattering cross section (C_{sca}). The slope of the C_{sca} measured by CAPS-ALB (or the Nephelometer) and modeled by Mie theory was close to 1 (Fig. S5), indicating the reliability of the CAPS-ALB and Nephelometer.***"**

[Comment 13] Line 127: "a" in front of "single". Also, what do the authors mean by "without any assumptions"?

Response: We thank the reviewer for pointing this out. We have corrected the sentence to include the article "a" before "single BC-containing particle." In addition, we clarified the meaning of "without any assumptions" as follows (Lines 176-178):

"*Under the assumption of singly charged particles, the mixing state of a single BC-containing particle can be represented by the mass ratio of the BC coating to the BC core, without relying on assumptions about particle morphology or coating structure,"*

[Comment 14] Line 129: "to compare the" -> "to be compared with"

Response: Corrected.

[Comment 15] Line 134: Mie is good only for spherically symmetric particles. How do the authors account for that, considering the premise of the paper is the deviation from spherical symmetry?

Response: We thank the reviewer for this insightful comment. We fully agree that Mie theory strictly applies to spherically symmetric particles, whereas ambient BC-containing particles often deviate from this idealized assumption. In our analysis, Mie theory was used to obtain the theoretical scattering cross section ($C_{sca\_modeled}$) under the core-shell approximation. To account for discrepancies between modeled and measured C_{sca}, we fitted the relationship between the $C_{sca\_measured}$ and M_R, and applied this fit in the calculation of absorption. This approach effectively includes BC particles whose optical properties are not captured by the core-shell Mie model, including those with eccentric core-shell structures. The revised description can be found at Lines 464-473.

"*In this study, we introduce an observationally constrained parameterization that links SP2-measured scattering cross sections with core-shell Mie calculations. This scheme identifies the optical transition state through following steps: (1) measuring single-particle C_{sca} with SP2, (2) fitting the relationship between $C_{sca\_measured}$ and M_R (Fig. 4b-4c), (3) identifying the M_R range associated with transitional optical behavior ("transition state"), and (4) inferring the MAC of transition-state particles using the fitted relationship before integrating MAC over all particles to obtain bulk E_{abs}. This parameterization improves agreement with observations, especially during clean periods (Case 1), when the uniform core-shell assumption tends to produce the largest discrepancies.*"

[Comment 16] Line 137: The refractive index used here seems quite high with respect to other studies in the literature. Additionally, the coating is sometimes slightly absorbing, and that can make a difference, especially at shorter wavelengths. A sensitivity analysis using a range of indices of refraction would be helpful.

Response: We thank the reviewer for this comment. In this study, the refractive indices were chosen primarily to derive the M_R-dependent optical transition behavior of BC-containing particles from SP2 scattering measurements at 1064 nm. The BC core is assigned a complex refractive index of 2.26-1.26i, while the non-absorbing coating has a refractive index of 1.48 and a density of 1.5 g cm^{-3}, values that have been widely used in previous studies (Liu et al., 2017a; Zhao et al., 2020; Liu et al., 2015). Besides, since the coating in this work does not absorb at 1064 nm, its potential absorption

can be safely neglected for the purpose of deriving the M_R-dependent optical transition behavior. To make our purpose clearer to the readers, the main text has been revised as follows (Lines 190-209):

"*The M_R-dependent optical transitions of BC-containing particles were further derived from SP2 measurements at a wavelength of 1064 nm. In the CPMA-SP2 system, when both M_p and M_{BC_core} are known, the modeled scattering cross section ($C_{sca\_modeled}$) of BC-containing particles can be derived using Mie theory (Wang et al., 2021a). This calculation assumes a core-shell structure, with the BC core having a refractive index of 2.26-1.26i (Liu et al., 2017a; Zhao et al., 2020) and the non-absorbing coating characterized by a refractive index of 1.48 and a density of 1.5 g cm^{-3} at a wavelength of 1064 nm (Liu et al., 2015). The measured scattering cross section ($C_{sca\_measured}$) was obtained from the SP2 using the leading-edge-only (LEO) technique, which reconstructs the scattering signal as BC-containing particles pass through the SP2 laser beam due to partial evaporation of refractory-absorbing material. The validity of this reconstruction relies on the assumption that the leading-edge data used for fitting represents an unperturbed particle, as extensively reported in previous studies (Liu et al., 2014; Zhang et al., 2016; Brooks et al., 2019; Gao et al., 2007; Zhang et al., 2020). Note only particles with successfully fitted LEO signals are considered in the optical property calculations. By comparing $C_{sca\_measured}$ with $C_{sca\_modeled}$, the M_R-dependent optical behavior of BC-containing particles can be inferred, particularly for transition-state particles. This comparison captures how variations in coating-to-core mass ratio influence scattering, providing observational constraints on the optical evolution of BC during aging (Liu et al., 2017a; Liu et al., 2020).*"

[Comment 17] Line 154: MAC units?

Response: We thank the reviewer for pointing this out. The unit of MAC has been clarified as m^2 g^{-1} and added to the Methods section (Line 220).

[Comment 18] Line 164: Why are these refractive index values different from those in Figure 137? Is it because of the wavelength? The wavelengths should be specified clearly in every instance.

Response: We thank the reviewer for pointing this out. The refractive index values differ from those in Line 195 because they correspond to different wavelengths. Here, our focus is on calculating the E_{abs} at 630 nm, which corresponds to the measurement wavelength of the CAPS instrument. We apologize for any confusion this may have caused and have clarified the wavelengths explicitly in the main text (Lines 236-240):

"*Given the measurement data available in this study, the Core-shell Mie theory was used to calculate the E_{abs} of BC-containing particles at a wavelength of 630 nm. The refractive index (RI) of BC and its coatings are assumed to be n=1.85+0.71i and n=1.5+0i at a wavelength of 630 nm (Liu et al., 2015; Liu et al., 2014).*"

[Comment 19] Figure 1: The core shell Mie model is for 200 nm, what is that a radius or a diameter, and is it mass equivalent, or something else? Also, why 200 nm exactly? More discussion on the model would be useful.

Response: We thank the reviewer for the comment. The 200 nm value in the Core-shell Mie model refers to the mass-equivalent diameter of the BC-containing particles, not the radius. The modeled E_{abs} of 200 nm mass-equivalent diameter was selected to illustrate the pronounced increase of BC

E_{abs} with increasing M_R in the Core-shell Mie model. To further support this conclusion and demonstrate the robustness of the trend, we have additionally included simulation results for 100 nm mass-equivalent diameter particles in Figure. 1. And some explanatory text has also been added to the figure caption.

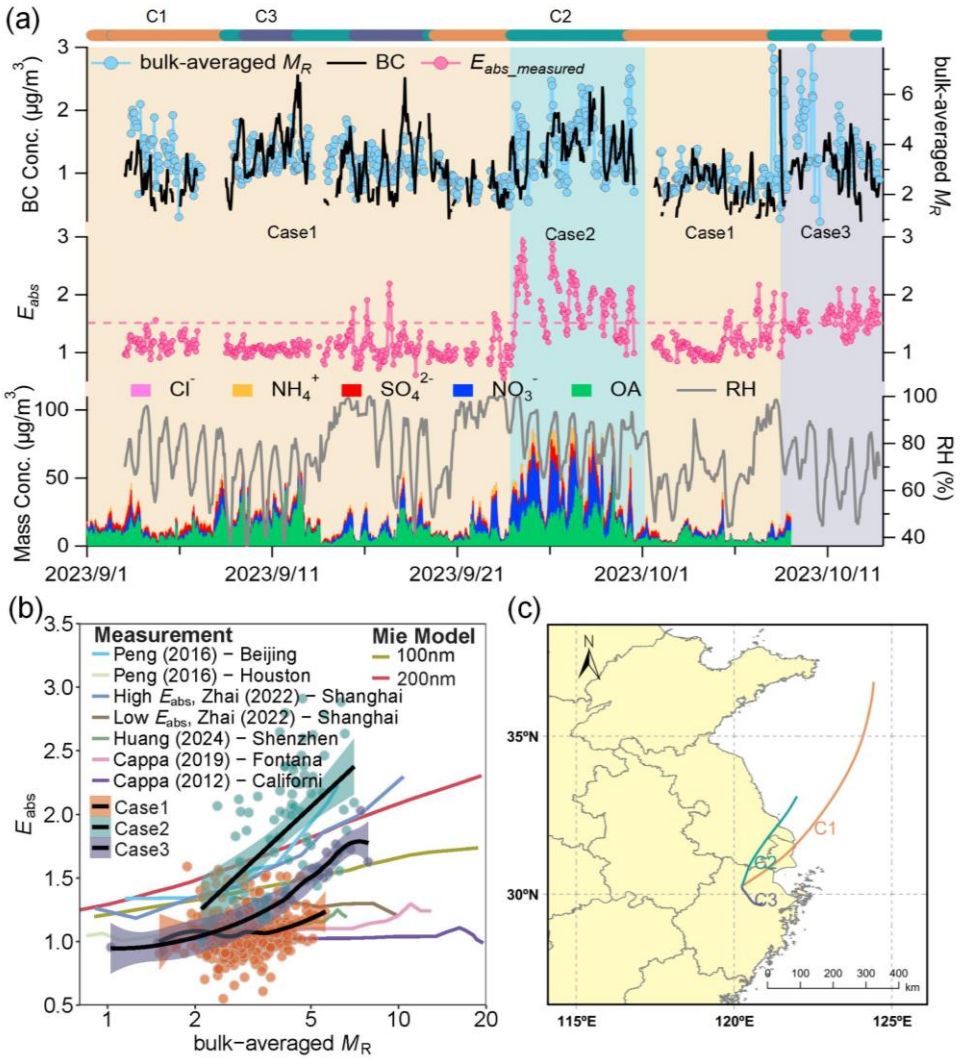

Figure. 1 *(a) The time series of BC concentrations, bulk-averaged M_R, measured E_{abs}, and the chemical components (including organics, nitrate, sulfate, ammonium and chloride) measured by TOF-ACSM X, as well as relatively humidity (RH). Shaded regions indicate different cases: light yellow for Case 1, blue-green for Case 2, and gray for Case 3. (b) Comparison of measured E_{abs} in different observation periods and with previous studies (Peng et al., 2016; Cappa et al., 2012; Zhai et al., 2022; Cappa et al., 2019; Huang et al., 2024). The black solid line represents the fitted smoothing curve of bulk-averaged M_R and measured E_{abs}, with the shaded area indicating the 95% confidence interval of the fit. (c) Mean 48-h back-trajectory simulations initialized at 100 m above ground level. The back trajectories were calculated using the Hybrid Single-Particle Lagrangian Integrated Trajectory (HYSPLIT) model driven by GDAS meteorological fields.*

[Comment 20] Line 215: I would not use the word "closely" here; the agreement is reasonable, but not that close.

Response: We thank the reviewer for the suggestion. This sentence has been revised in the

manuscript to replace "closely matches" with "reasonably agrees" (Lines 293-295).

"*On the other hand, in Case 2, the E_{abs} calculated using the traditional core-shell Mie model ($E_{abs\_uniform}$) reasonably agrees with the $E_{abs\_measured}$, whereas Case 3 shows a slightly lower level of consistency.*"

[Comment 21] Line 227: What does "at different period" refer to exactly? Perhaps "periods".

Response: We appreciate the reviewer's suggestion. The phrase "at different period" has been corrected to "at different periods" for grammatical accuracy, and we have clarified that it refers to different observation (or clean/polluted) periods in the revised manuscript (Lines 318-320).

"*Fig. 2a and 2b illustrated significant differences in the normalized number distribution of BC-containing particles at M_p = 4.35 fg and 9.38 fg during different observation periods.*"

[Comment 22] Line 232: Why log10?

Response: We appreciate the reviewer's insightful question. The logarithmic transformation of M_R ($\log_{10}(M_R)$) was applied to reduce the strong skewness in the M_R distribution, which typically spans several orders of magnitude. Using $\log_{10}(M_R)$ allows the data to approximate a normal distribution, making the standard deviation a more representative measure of heterogeneity. This approach is also consistent with previous studies (Fierce et al., 2020; Huang et al., 2024).

[Comment 23] Line 241-242: I am not sure what "due to stems" means.

Response: We thank the reviewer for pointing out this grammatical mistake. The phrase "due to stems from" was indeed redundant and has been corrected in the revised manuscript (Lines 336-337):

"Such discrepancies likely due to the uniform core-shell model's simplified treatment of M_R heterogeneity in BC (Romshoo et al., 2024; Wang et al., 2021b)."

[Comment 24] Lines 264-265: I am not clear how these ranges are defined.

Response: We thank the reviewer for this suggestion. In this study, the M_R range defining the "transition state" was determined based on the variation of $C_{sca\_measured}/C_{sca\_modeled}$ with M_R. Specifically, the lower boundary corresponds to the M_R value at which the ratio begins to increase after an initial decrease, while the upper boundary corresponds to the M_R value where the ratio approaches 1. We hope this explanation helps clarify our definition.

[Comment 25] Line 265: I do not recall the authors discussing the pollution regimes of the three cases. I would give that more emphasis early on because that is probably at the root of the observed behaviors.

Response: We thank the reviewer for this helpful comment. We would like to clarify that the pollution regimes of the three cases have been analyzed in both the beginning of Section 3 and in the concluding part of the discussion. Specifically, we examined the differences in air-mass origins and chemical composition for the three cases, as shown in Lines 265-282 and Lines 363-370:

Lines 265-282: "*To investigate the temporal evolution of BC coating, the observation period was classified into three cases based on the variation of $E_{abs\_measured}$, using E_{abs}=1.5 as the reference*

threshold (Fig.1). Case 1 (September 3-23 and October 1-7, 2023) corresponds to $E_{abs\_measured}$ significantly below 1.5. These periods were characterized by relatively low non-refractory PM_1 concentrations and high wind speeds (WS = 0.94 ± 0.04 m/s). Back-trajectory analysis further shows that Case 1 was dominated by clean marine and nearby local air masses, resulting in relatively clean and weakly aged conditions (Fig. 1a). Case 2 (September 24–30) corresponds to periods when $E_{abs\_measured}$ remained continuously higher than 1.5. This episode occurred under stagnant meteorological conditions-characterized by weak winds (WS = 0.81 ± 0.02 m/s) and elevated relative humidity (RH = 81.34 ± 17.12%) -that favored secondary aerosol formation. Back-trajectory analysis further indicates that Case 2 was dominated by air masses transported from Jiangsu and passing through northern Zhejiang, enhancing pollutant accumulation and promoting more aged BC conditions. Case 3 includes periods when $E_{abs\_measured}$ persistently fluctuated around 1.5. The air masses during this period were a mixture of polluted inland outflow and clean marine inflow, suggesting the air masses were moderately aged–which explains the intermediate E_{abs}."

Lines 363-370: "*The higher M_R thresholds observed in Case 2 and Case 3 indicate that under polluted conditions, BC particles can reach an optically core-shell-like state with comparatively less coating material. This likely reflected accelerated aging driven by enhanced secondary formation and condensation of inorganics and organics on BC, facilitated by stagnant meteorological conditions (low wind speed). Such conditions promote efficient coating growth on BC-containing particles, strengthening their light-absorption capability and leading to high E_{abs}. Therefore, compared with Case 1, BC in Case 2 and Case 3 required less coating material to reach the core-shell configuration.*"

[Comment 26] Line 269: What do the authors mean by heterogeneous aging?

Response: We thank the reviewer for pointing out this unclear expression. We apologize for the ambiguity. In this context, "heterogeneous aging" refers to the evolution of heterogeneity among BC-containing particles during their aging process, such as differences in coating degrees or mixing states that develop over time. To avoid confusion, this part has been fully revised and integrated into other related sections. The updated content can be found in Lines 363-370 of the revised manuscript.

"*The higher M_R thresholds observed in Case 2 and Case 3 indicate that under polluted conditions, BC particles can reach an optically core-shell-like state with comparatively less coating material. This likely reflected accelerated aging driven by enhanced secondary formation and condensation of inorganics and organics on BC, facilitated by stagnant meteorological conditions (low wind speed). Such conditions promote efficient coating growth on BC-containing particles, strengthening their light-absorption capability and leading to high E_{abs}. Therefore, compared with Case 1, BC in Case 2 and Case 3 required less coating material to reach the core-shell configuration.*"

[Comment 27] Line 272: While plausible, this explanation (on why "BC required less coating material to evolve into a core-shell structure") is not completely clear to me, and the authors might want to elaborate more.

Response: We thank the reviewer for this valuable comment and apologize for the lack of clarity in our previous explanation. We have revised this part to provide a more detailed and explicit discussion. The updated content can be found in Lines 367-370 of the revised manuscript.

"*The higher M_R thresholds observed in Case 2 and Case 3 indicate that under polluted conditions,*

BC particles can reach an optically core-shell-like state with comparatively less coating material. This likely reflected accelerated aging driven by enhanced secondary formation and condensation of inorganics and organics on BC, facilitated by stagnant meteorological conditions (low wind speed). Such conditions promote efficient coating growth on BC-containing particles, strengthening their light-absorption capability and leading to high E_{abs}. Therefore, compared with Case 1, BC in Case 2 and Case 3 required less coating material to reach the core-shell configuration."

[Comment 28] Line 292: Again, I think "closely" is too strong.

Response: We have revised the sentence to avoid overstatement, changing "closely aligns with" to "agrees with." (Lines 389)

[Comment 29] Lines 300-302: I believe in the paper by Fierce et al., the discrepancy was suggested to be due to MR heterogeneity but mostly for Large coatings, while for low coatings the deviations were associated with non-core-shell configurations, so I do not see a clear discrepancy between the two studies, on the contrary, it seems to me that the results are quite similar when considered for similar coating regimes.

Response: We thank the reviewer for this comment. We agree that the interpretation in Fierce et al. (2020) depends on the coating conditions, and that our results are generally consistent with their findings when similar coating levels are considered. In our study, the relatively larger deviation observed for Case 1, compared to previous particle-resolved modeling studies, is primarily due to the smaller standard deviation of particle-to-particle M_R in our observations, which leads to a greater discrepancy between measured and modeled E_{abs}. This explanation has been clarified in the revised manuscript (Lines 396-401).

"*The results show that for Case 1, although the discrepancy between the measured and modeled values exhibits a decreasing trend, the average deviation remains as high as 38%. This larger deviation, compared to previous particle-resolved modeling studies, is primarily attributed to the smaller dispersion of particle-to-particle M_R observed in Case 1 (Fig. 2c) relative to their model simulations (Fierce et al., 2020).*"

[Comment 30] Figure 4(b), 4(c), and 4(d), what is on the x axis? Please put an axis title and units if applicable.

Response: We thank the reviewer for pointing this out. Axis labels and units have been added to Figures 4(b), 4(c), and 4(d) for clarity. Specifically, the x-axis represents M_R ranges corresponding to "transition-state" BC-containing particles, which is now clearly indicated in the revised figures.

[Comment 31] Line 323: Why inorganic specifically? Why not also organics?

Response: We thank the reviewer for this comment. In response to feedback from multiple reviewers, we have thoroughly revised the discussion in this section to clarify the factors influencing E_{abs} considering both inorganic and organic coatings. Our analysis indicates that among the different aerosol chemical components examined, the E_{abs} increases systematically only with the increasing contribution of secondary nitrate, whereas variations in other components show no significant effect. These findings are now fully reflected in the revised manuscript, which provides a more comprehensive and data-supported interpretation (Lines 415-457).

"*The transitional-state particles are BC-containing particles in the process of evolving from loosely aggregated fractal-like structures toward quasi–core–shell configurations (Moffet et al., 2016; Moteki and Kondo, 2007). The abundance of transitional-state particles varies notably under different atmospheric conditions, directly influencing the measured E_{abs} (Liu et al., 2017a). During clean days (Case 1), the atmospheric environment was characterized by low PM_1 concentrations, weak secondary formation, and highly variable coating conditions. Under such conditions, our measurements show that BC-containing particles were dominated by transitional-state structures (Fig. S9), representing the intermediate stage between externally mixed aggregates and fully developed quasi–core–shell structures. The limited and heterogeneous coating distribution on these particles substantially weakens the lensing effect, resulting in lower measured E_{abs} (Peng et al., 2016). Because the core-shell Mie model inherently assumes a uniform and concentric coating, it does not accurately represent the optical behavior of these transitional particles, leading to a pronounced overestimation of measured E_{abs} during Case 1. This indicates that, under clean conditions, the optical properties of transitional-state particles are the key driver of the model-observation discrepancy. In contrast, the haze period (Case 2) represents a more aged and heavily coated aerosol environment and provides a useful reference for understanding the factors influencing the measured E_{abs}. During Case 2, the high aerosol loading and elevated bulk-averaged M_R were largely influenced by regional transport, as air masses at 100 m, 500 m, and 1000 m all followed similar pathways from the northern Yangtze River Delta into northern Zhejiang (Fig. 1c and Fig. S7). Stagnant meteorological conditions, elevated relative humidity, and enhanced oxidative capacity further facilitated vigorous liquid-phase and photochemical reactions, promoting the abundant formation of secondary coatings on BC surfaces (Peng et al., 2016). Notably, our observations show that E_{abs} increases systematically with the increasing contribution of secondary nitrate (Fig. S8), consistent with the fact that nitrate-rich conditions enhance aqueous-phase oxidation and accelerate the formation of thick inorganic coatings (Liu et al., 2017b). As a result, a much larger fraction of BC-containing particles exhibited internally mixed, quasi–core-shell structures rather than transitional states (Fig. S9), which explains why the core-shell Mie model performs substantially better for Case 2 than for Case 1. This contrast reinforces the central role of transitional-state particles in determining measured E_{abs} when coatings are sparse, irregular, or partially developed. Given the strong influence of transitional-state particles on measured E_{abs} in Case 1, precise constraints on their optical behavior are crucial for improving E_{abs} estimates across different atmospheric scenarios. To address this, an empirical formula based on optical measurements was developed to estimate the E_{abs} of BC-containing particles in the "transition state", derived from fitting the measured C_{sca} against M_R (Fig. 3d-3f). By applying this empirical formula to the calculation of E_{abs}, the resulting value for Case 1 was 1.21 ± 0.01. For Case 2 and Case 3, the E_{abs} calculated using the same formula (E_{abs_param}) remained slightly lower than the $E_{abs\_measured}$, but the deviation was within 20%, demonstrating the reliability of the approach across different atmospheric conditions.*"

[Comment 32-33] Line 337: The authors should clearly describe the "improved method". Here, it is not clear at all what that is. How was the fit performed, and what did they do with the fit?

Lines 360 to 368: How do the authors suggest developing such a unified model?

Response: We thank the reviewer for these comments. Both points regarding the "improved method" and the development of a unified model have been fully addressed in **[Comment 5]**, where we

provide a detailed description of the observationally constrained parameterization, including how the $C_{sca\_measured}$-M_R fit is performed, how the fit is used to estimate E_{abs} for transition-state particles, and how the framework can be adapted for different atmospheric conditions. Please refer to **[Comment 5]** for the complete explanation.

[Comment 34] Figure S2: It is not clear how the CPC would measure a size distribution, being a simple counter. The caption mentions a DMA; perhaps that should be clearer from the legend. What are SCHG and BBHG (scattering and broadband high gain?). Spell out acronyms in the caption.

Response: We thank the reviewer for this helpful comment. We have clarified in the figure caption that the size distribution was measured using a DMA coupled with a CPC. In addition, the acronyms SCHG and BBHG have been spelled out as scattering high gain and broadband high gain, respectively. The legend and caption have been revised in revised Supporting Information.

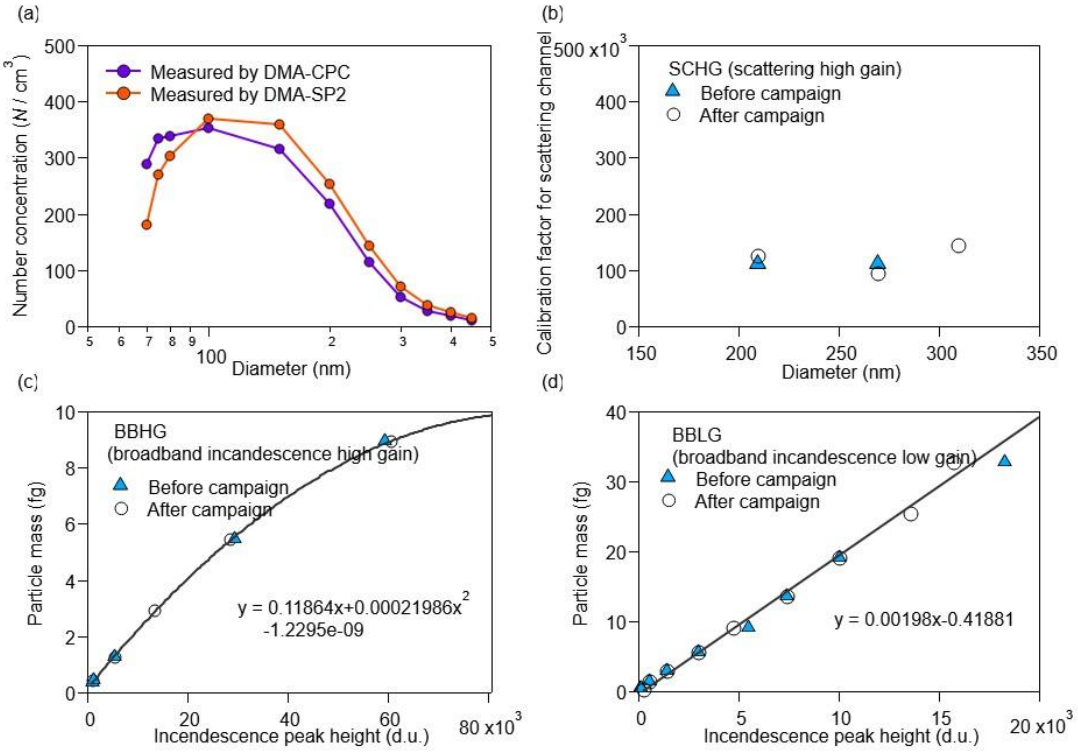

Figure S2*. The number concentration measured by SP2 and CPC after DMA classification of size-resolved Aquadag aerosols (a). (b) showed the calibration factor for scattering high gain (SCHG) before and after campaign. (c) and (d) display the correlation between incandescence peak height and BC particle mass at broadband incandescence high gain (BBHG) and broadband incandescence low gain (BBLG), respectively.*

[Comment 35] Figures S4 and S5: the signal ranges are very different. Why is that? Can the nephelometer and the CAPS measure scattering coefficients below 0.01 Mm-1 accurately and precisely? That is hard to believe. Also how were the Mie simulations being informed, in terms of concentrations, size, and index of refraction?

Response: We thank the reviewer for these valuable comments. The apparent difference in signal ranges between Figures S4 and S5 was due to a labeling error in Figure S5. The unit should be scattering cross section (m^2) rather than scattering coefficient (Mm^{-1}), and this has been corrected

in the revised Supplementary Information.

[Comment 36] Figure S7: What does the horizontal pink dashed line indicate, the mean Eabs?

Response: We thank the reviewer for the comment. The horizontal pink dashed lines represent the upper and lower bounds of the 90% confidence interval of the fitted curve, which were automatically calculated by Igor based on the fit. This has been clarified in the figure caption in the revised Supplementary Information (see Figure S6).

[Comment 37] Figure S8: Some more information is needed. How were the trajectories being calculated? What is the time span, what is the elevation used, can the authors also provide vertical trajectories to see whether the air masses are coming from the boundary layer or from aloft to understand if it is near or long-range transportation?

Response: We thank the reviewer for this comment. To improve clarity, we have merged the original Figure S8 with Figure 1 in the revised manuscript (see **[Comment 19]**). The back trajectories were calculated using the HYSPLIT model driven by GDAS meteorological fields. In the updated Figure 1, we show 48-hour backward trajectories initialized at 100 m above ground level. To further examine the vertical representativeness and to assess whether the air masses originate from the boundary layer or from higher altitudes, additional trajectories initialized at 500 m and 1000 m (also for 48 hours) are now provided in Figure S7. These additional simulations demonstrate that the air-mass pathways are similar across different starting altitudes, supporting our interpretation of the transport characteristics.

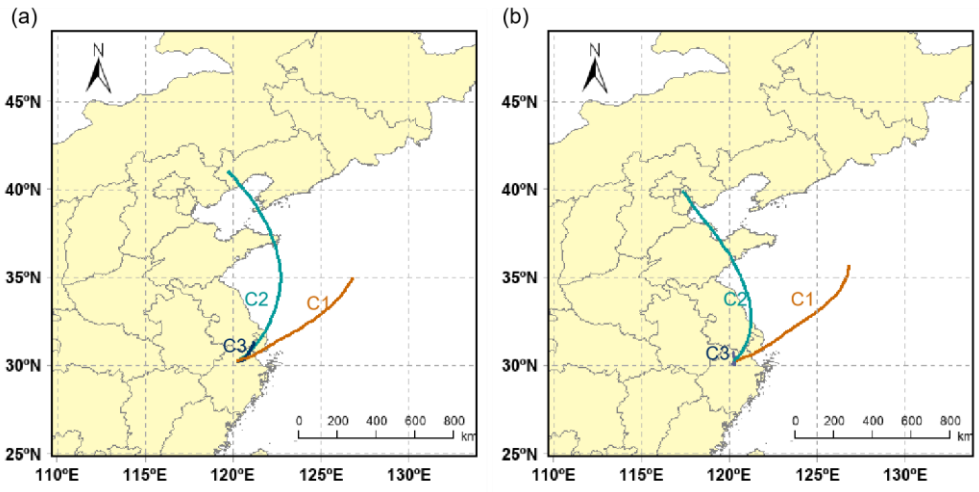

Figure S7. *48-hour backward trajectories of air masses during all observation periods at 100 m, 500 m, and 1000 m above ground level, calculated using the Hybrid Single-Particle Lagrangian Integrated Trajectory (HYSPLIT) model driven by GDAS meteorological fields.*

[Comment 38] Figure S9: Are these based on the SP2?

Response: We thank the reviewer for the comment. Yes, the data in Figure S9 are based on SP2 measurements, and this has been explicitly indicated in the figure title in the revised Supplementary Information (Figure S9).

[Comment 39] Figure S10: The units on the x-axis are not critical, but still, it would be nice to have

them.

Response: We thank the reviewer for the comment. In response to this and other reviewers' suggestions, we have supplemented the distributions of scattering signals for all M_p and added the units on the x-axis. The updated figure is now presented as Figure S11 in the revised Supplementary Information.

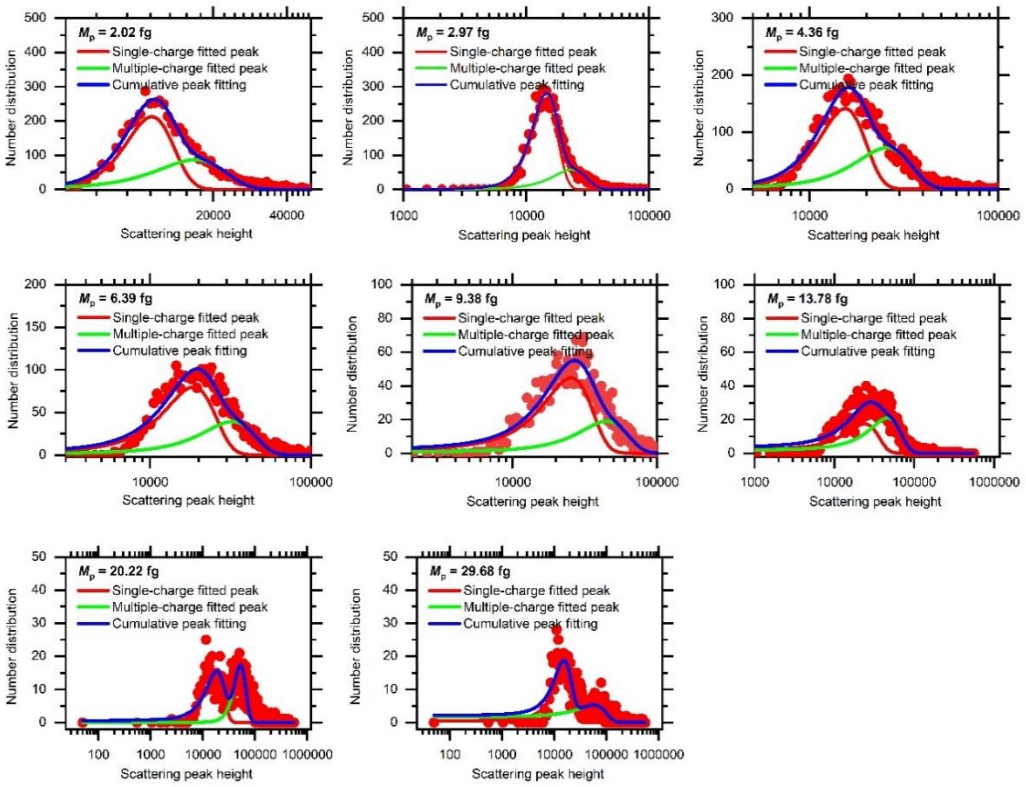

***Figure S11**. Multiple charging diagnostics in the tandem CPMA-SP2 system. The number distribution of scattering-signal peak heights at each selected M_p was fitted using a bimodal Gaussian function, with one peak representing singly charged particles and the other corresponding to doubly charged particles. The intersection point of the two fitted peaks was used as the threshold for distinguishing singly from doubly charged particles at that M_p, enabling a quantitative evaluation of multiple charging effects.*

[Comment 40] Figure S11: Units on x axes (fg?).

Response: In response to the comment, the units on the x-axis have been added as fg. The updated figure is now presented as Figure S12 in the revised Supplementary Information.

[Comment 41] Some limited references that might be of relevance:

1. Beeler, P., et al., Light absorption enhancement of black carbon in a pyrocumulonimbus cloud. Nature Communications, 2024. 15(1): p. 6243.

2. Ueda, S., et al., Light absorption and morphological properties of soot-containing aerosols observed at an East Asian outflow site, Noto Peninsula, Japan. Atmos. Chem. Phys., 2016. 16(4): p. 2525-2541.

3. China, S., et al., Morphology and mixing state of individual freshly emitted wildfire carbonaceous particles. Nature Communications, 2013. 4.

4. Cross, E.S., et al., Soot Particle Studies—Instrument Inter-Comparison—Project Overview. Aerosol Science and Technology, 2010. 44(8): p. 592-611.
5. Corbin, J.C., R.L. Modini, and M. Gysel-Beer, Mechanisms of soot-aggregate restructuring and compaction. Aerosol Science and Technology, 2022: p. 1-48.
6. Adachi, K. and P.R. Buseck, Changes of ns-soot mixing states and shapes in an urban area during CalNex. Journal of Geophysical Research: Atmospheres, 2013. 118(9): p. 3723–3730.
7. Adachi, K., S.H. Chung, and P.R. Buseck, Shapes of soot aerosol particles and implications for their effects on climate. Journal of Geophysical Research-Atmospheres, 2010. 115.
8. Adachi, K., et al., Mixing states of light-absorbing particles measured using a transmission electron microscope and a single-particle soot photometer in Tokyo, Japan. Journal of Geophysical Research: Atmospheres, 2016. 121(15): p. 9153-9164.
9. leviChang, H. and T.T. Charalampopoulos, Determination of the Wavelength Dependence of Refractive-Indexes of Flame Soot. Proceedings of the Royal Society-Mathematical and Physical Sciences, 1990. 430(1880): p. 577-591.
10. Moteki, N., Measuring the complex forward-scattering amplitude of single particles by self-reference interferometry: CAS-v1 protocol. Optics Express, 2021. 29(13): p. 20688-20714.
11. Liu, S., et al., Enhanced light absorption by mixed source black and brown carbon particles in UK winter. Nat Commun, 2015. 6.

Response: We thank the reviewer for providing these references. The manuscript has been thoroughly revised, and most of the suggested references have already been incorporated. A few references (specifically references 4, 9 and 10) were not cited, as their focus is not directly aligned with the objectives of the present study.

References:

Adachi, K. and Buseck, P. R.: Changes of ns-soot mixing states and shapes in an urban area during CalNex, Journal of Geophysical Research-Atmospheres, 118, 3723-3730, 10.1002/jgrd.50321, 2013.

Adachi, K., Chung, S. H., and Buseck, P. R.: Shapes of soot aerosol particles and implications for their effects on climate, Journal of Geophysical Research: Atmospheres, 115, D15206, 10.1029/2009jd012868, 2010.

Brooks, J., Liu, D., Allan, J. D., Williams, P. I., Haywood, J., Highwood, E. J., Kompalli, S. K., Babu, S. S., Satheesh, S. K., Turner, A. G., and Coe, H.: Black carbon physical and optical properties across northern India during pre-monsoon and monsoon seasons, Atmospheric Chemistry and Physics, 19, 13079-13096, 10.5194/acp-19-13079-2019., 2019.

Cappa, C. D., Zhang, X., Russell, L. M., Collier, S., Lee, A. K. Y., Chen, C. L., Betha, R., Chen, S., Liu, J., Price, D. J., Sanchez, K. J., McMeeking, G. R., Williams, L. R., Onasch, T. B., Worsnop, D. R., Abbatt, J., and Zhang, Q.: Light Absorption by Ambient Black and Brown Carbon and its Dependence on Black Carbon Coating State for Two California, USA, Cities in Winter and Summer, Journal of Geophysical Research: Atmospheres, 124, 1550-1577, 10.1029/2018JD029501, 2019.

Cappa, C. D., Onasch, T. B., Massoli, P., Worsnop, D. R., Bates, T. S., Cross, E. S., Davidovits, P., Hakala, J., Hayden, K. L., Jobson, B. T., Kolesar, K. R., Lack, D. A., Lerner, B. M., Li, S.-M., Mellon, D., Nuaaman, I., Olfert, J. S., Petäjä, T., Quinn, P. K., Song, C., Subramanian, R., Williams, E. J., and Zaveri, R. A.: Radiative Absorption Enhancements Due to the Mixing State of Atmospheric Black

Carbon, Science, 337, 1078-1081, https://doi.org/10.1126/science.1223447, 2012.

China, S., Mazzoleni, C., Gorkowski, K., Aiken, A. C., Dubey, M. K., and Michigan Technological Univ, H. M. I.: Morphology and mixing state of individual freshly emitted wildfire carbonaceous particles, Nature Communications, 4, 2122-2122, 10.1038/ncomms3122, 2013.

Corbin, J. C., Modini, R. L., and Gysel-Beer, M.: Mechanisms of soot-aggregate restructuring and compaction, Aerosol Science and Technology, 57, 89-111, 10.1080/02786826.2022.2137385, 2023.

Fierce, L., Onasch, T. B., Cappa, C. D., Mazzoleni, C., China, S., Bhandari, J., Davidovits, P., Al Fischer, D., Helgestad, T., Lambe, A. T., Sedlacek, A. J., Smith, G. D., Wolff, L., Brookhaven National Lab, U. N. Y., and Pacific Northwest National Lab, R. W. A.: Radiative absorption enhancements by black carbon controlled by particle-to-particle heterogeneity in composition, Proceedings of the National Academy of Sciences, 117, 5196-5203, 10.1073/pnas.1919723117, 2020.

Gao, R. S., Schwarz, J. P., Kelly, K. K., Fahey, D. W., Watts, L. A., Thompson, T. L., Spackman, J. R., Slowik, J. G., Cross, E. S., Han, J. H., Davidovits, P., Onasch, T. B., and Worsnop, D. R.: A Novel Method for Estimating Light-Scattering Properties of Soot Aerosols Using a Modified Single-Particle Soot Photometer, Aerosol Science and Technology, 41, 125-135, 10.1080/02786820601118398, 2007.

Huang, X.-F., Peng, Y., Wei, J., Peng, J., Lin, X.-Y., Tang, M.-X., Cheng, Y., Men, Z., Fang, T., Zhang, J., He, L.-Y., Cao, L. M., Liu, C., Zhang, C., Mao, H., Seinfeld, J. H., and Wang, Y.: Microphysical complexity of black carbon particles restricts their warming potential, One Earth, 7, 10.1016/j.oneear.2023.12.004, 2024.

Liu, D., Taylor, J. W., Young, D. E., Flynn, M. J., Coe, H., and Allan, J. D.: The effect of complex black carbon microphysics on the determination of the optical properties of brown carbon: BC morphology on BrC optical properties, Geophysical Research Letters, 42, 613-619, 10.1002/2014GL062443, 2015.

Liu, D., Allan, J. D., Young, D. E., Coe, H., Beddows, D., Fleming, Z. L., Flynn, M. J., Gallagher, M. W., Harrison, R. M., Lee, J., Prevot, A. S. H., Taylor, J. W., Yin, J., Williams, P. I., and Zotter, P.: Size distribution, mixing state and source apportionment of black carbon aerosol in London during wintertime, Atmospheric Chemistry and Physics, 14, 10061-10084, 10.5194/acp-14-10061-2014, 2014.

Liu, D., Whitehead, J., Alfarra, M. R., Reyes-Villegas, E., Spracklen, D. V., Reddington, C. L., Kong, S., Williams, P. I., Ting, Y.-C., Haslett, S., Taylor, J. W., Flynn, M. J., Morgan, W. T., McFiggans, G., Coe, H., and Allan, J. D.: Black-carbon absorption enhancement in the atmosphere determined by particle mixing state, Nature Geoscience, 10, 184-188, 10.1038/ngeo2901, 2017a.

Liu, H., Pan, X., Liu, D., Liu, X., Chen, X., Tian, Y., Sun, Y., Fu, P., and Wang, Z.: Mixing characteristics of refractory black carbon aerosols at an urban site in Beijing, Atmospheric Chemistry and Physics, 20, 5771-5785, 10.5194/acp-20-5771-2020, 2020.

Liu, Y., Wu, Z., Wang, Y., Xiao, Y., Gu, F., Zheng, J., Tan, T., Shang, D., Wu, Y., Zeng, L., Hu, M., Bateman, A. P., and Martin, S. T.: Submicrometer Particles Are in the Liquid State during Heavy Haze Episodes in the Urban Atmosphere of Beijing, China, Environmental Science & Technology Letters, 4, 427-432, 10.1021/acs.estlett.7b00352, 2017b.

Moffet, R. C., O'Brien, R. E., Alpert, P. A., Kelly, S. T., Pham, D. Q., Gilles, M. K., Knopf, D. A., Laskin, A., Pacific Northwest National Lab, R. W. A. E. M. S. L., Lawrence Berkeley National Lab, B. C. A., and Stony Brook Univ, S. B. N. Y.: Morphology and mixing of black carbon particles collected in central California during the CARES field study, Atmospheric chemistry and physics, 16, 14515-

14525, 10.5194/acp-16-14515-2016, 2016.

Moteki, N. and Kondo, Y.: Effects of Mixing State on Black Carbon Measurements by Laser-Induced Incandescence, Aerosol Science and Technology, 41, 398-417, 10.1080/02786820701199728, 2007.

Peng, J., Hu, M., Guo, S., Du, Z., Zheng, J., Shang, D., Zamora, M. L., Zeng, L., Shao, M., Wu, Y.-S., Zheng, J., Wang, Y., Glen, C. R., Collins, D. R., Molina, M. J., and Zhang, R.: Markedly enhanced absorption and direct radiative forcing of black carbon under polluted urban environments, Proceedings of the National Academy of Sciences, 113, 4266-4271, 10.1073/pnas.1602310113, 2016.

Romshoo, B., Müller, T., Ahlawat, A., Wiedensohler, A., Haneef, M. V., Imran, M., Warsi, A. B., Mandariya, A. K., Habib, G., and Pöhlker, M. L.: Significant contribution of fractal morphology to aerosol light absorption in polluted environments dominated by black carbon (BC), npj Climate and Atmospheric Science, 7, 87, 10.1038/s41612-024-00634-0, 2024.

Wang, T. T., Zhao, G., Tan, T. Y., Yu, Y., Tang, R. Z., Dong, H. B., Chen, S. Y., Li, X., Lu, K. D., Zeng, L. M., Gao, Y. Q., Wang, H. L., Lou, S. R., Liu, D. T., Hu, M., Zhao, C. S., and Guo, S.: Effects of biomass burning and photochemical oxidation on the black carbon mixing state and light absorption in summer season, Atmospheric Environment, 248, 10.1016/j.atmosenv.2021.118230, 2021a.

Wang, Y., Li, W., Huang, J., Liu, L., Pang, Y., He, C., Liu, F., Liu, D., Bi, L., Zhang, X., and Shi, Z.: Nonlinear Enhancement of Radiative Absorption by Black Carbon in Response to Particle Mixing Structure, Geophysical Research Letters, 48, 10.1029/2021gl096437, 2021b.

Zhai, J., Yang, X., Li, L., Bai, B., Liu, P., Huang, Y., Fu, T.-M., Zhu, L., Zeng, Z., Tao, S., Lu, X., Ye, X., Wang, X., Wang, L., and Chen, J.: Absorption Enhancement of Black Carbon Aerosols Constrained by Mixing-State Heterogeneity, Environmental Science & Technology, 56, 1586-1593, 10.1021/acs.est.1c06180, 2022.

Zhang, F., Shen, J., Xu, D., Shen, J., Qin, Y., Shi, R., Wei, J., Xu, Z., Pei, X., Tang, Q., Chen, H., Xu, B., and Wang, Z.: Unveiling the key drivers and formation pathways for secondary organic aerosols in an eastern China megacity, Journal of Hazardous Materials, 498, 10.1016/j.jhazmat.2025.139925, 2025.

Zhang, Y., Zhang, Q., Cheng, Y., Su, H., Kecorius, S., Wang, Z., Wu, Z., Hu, M., Zhu, T., Wiedensohler, A., and He, K.: Measuring the morphology and density of internally mixed black carbon with SP2 and VTDMA: new insight into the absorption enhancement of black carbon in the atmosphere, Atmospheric Measurement Techniques, 9, 1833-1843, 10.5194/amt-9-1833-2016, 2016.

Zhang, Y. X., Zhang, Q., Yao, Z. L., and Li, H. Y.: Particle Size and Mixing State of Freshly Emitted Black Carbon from Different Combustion Sources in China, Environmental Science & Technology, 54, 7766-7774, 10.1021/acs.est.9b07373, 2020.

Zhao, G., Shen, C., and Zhao, C.: Technical note: Mismeasurement of the core-shell structure of black carbon-containing ambient aerosols by SP2 measurements, Atmospheric Environment, 243, 117885, 10.1016/j.atmosenv.2020.117885, 2020.